Group 11 complexes with the bis(3,5-dimethylpyrazol-1-yl)methane ligand. How secondary bonds can influence the coordination environment of Ag(I): the role of coordinated water in $[Ag_2(\mu\text{-}L)_2(OH_2)_2](OTf)_2$†‡

Maria José Calhorda,[b] Paulo J. Costa,[b] Olga Crespo,[a] M. Concepción Gimeno,*[a] Peter G. Jones,[c] Antonio Laguna,[a] Mar Naranjo,[a] Susana Quintal,[b] Yu-Jun Shi[a] and M. Dolores Villacampa[a]

Received 7th April 2006, Accepted 23rd May 2006
First published as an Advance Article on the web 27th June 2006
DOI: 10.1039/b605034d

The complexation properties of the ligand bis(3,5-dimethylpyrazol-1-yl)methane (**L**) towards group 11 metals have been studied. The reaction in a 1 : 1 molar ratio with $[Cu(NCMe)_4]PF_6$ or Ag(OTf) complexes gives the mononuclear $[CuL(NCMe)]PF_6$ (**1**), with crystallographic mirror symmetry, or dinuclear $[Ag_2(\mu\text{-}L)_2](OTf)_2$ (**2**) (OTf = trifluoromethanesulfonate) in which the ligand bridges both silver centres, an unprecedented mode of coordination for this type of ligands. Compound **2** crystallizes with two water molecules and forms a supramolecular structure through classical hydrogen bonding. The reaction in a 2 : 1 ratio affords in both cases the four-coordinated derivatives $[ML_2]X$ (M = Cu, X = PF_6 (**3**); Ag, X = OTf (**4**)). The treatment of $[Ag(OTf)(PPh_3)]$ with the ligand L gives $[AgL(PPh_3)]OTf$ (**5**). The gold(I) derivative $[Au_2(C_6F_5)_2(\mu\text{-}L)]$ (**6**) has also been obtained by reaction of L with two equivalents of $[Au(C_6F_5)(tht)]$. These complexes present a luminescent behaviour at low temperature; the emissions being mainly intraligand but enhanced after coordination of the metal. Compounds **1–4** have been characterized by X-ray crystallography. DFT studies showed that, in the silver complex **2**, coordination of H_2O to Ag in the binuclear complex is favoured by formation of a hydrogen-bonding network, involving the triflato anion, and releasing enough energy to allow distortion of the Ag_2 framework.

Introduction

Poly(pyrazol-l-yl)alkanes have been regarded as a very important class of multidentate nitrogen ligands since Trofimenko's initial report[1] and their coordination behaviour towards transition-metal complexes has been extensively investigated.[2,3] Bis(pyrazol-1-yl)methanes have been less studied than the corresponding tris(pyrazol-l-yl) ligands, but many derivatives have been reported in which this type of ligands coordinates in a bidentate chelate fashion to the metal centre.[4,5] The chemistry of group 11 metal complexes with the bis(pyrazol-1-yl)methanes is limited to copper and silver; no gold complex has been described. Silver(I) complexes are of the type $[AgL_2]^+$ (L = $RHC(pz)_2$ (R = Ph, CH_2Ph, py, Fc),[6–8] $R_2C(pz)_2$ (R = Me, Ph)),[6–9] in which the silver atom is tetra-coordinated, with the ligand acting as a bidentate chelate. Several copper(II) and copper(I) complexes have been reported recently and have the stoichiometry $[CuX_2L]$,[10] $[CuX_2L_2]$[11–17] or $[Cu_2(\mu\text{-}X)_2L_2]$[11,18] for Cu(II), and $[CuL_2]^+$,[10,11] or $[Cu_2(\mu\text{-}X)_2L_2]$[19,20] (X = halogen or pseudohalogen) for Cu(I). During the preparation of this manuscript, several copper(I) complexes of stoichiometry $[CuL_2]^+$, $[CuL(NCMe)_2]^+$ and $[CuL(NCMe)]^+$ (this complex being also described here with a different counteranion) have been published.[21]

Here we report on the synthesis of group 11 complexes with the ligand bis(3,5-dimethylpyrazol-1-yl)methane. The complexes with a M : L ratio of 1 : 1 are very different depending on the metal: for copper(I) the mononuclear $[CuL(NCMe)]PF_6$ is observed, for silver(I) the dinuclear $[Ag_2(\mu\text{-}L)_2](OTf)_2$, whereas the gold complex could not be isolated in a pure form. The silver derivative represents an unprecedented coordination mode obtained with this type of ligand in which the two silver atoms are bridged by the ligand and a short argentophilic Ag···Ag contact is present. A supramolecular structure arises from the formation of hydrogen bonds between the crystallizing water molecules and the triflate anions.

Results and discussion

Chemical studies and X-ray structures

The complexation properties of the ligand bis(3,5-dimethyl-pyrazol-1-yl)methane (**L**) towards group 11 metals have been studied. The reaction with the M^+ cations (as $[Cu(NCMe)_4]PF_6$ or Ag(OTf)) gives different results, depending on the metal (Scheme 1). For copper(I) the reaction in a 1 : 1 ratio gives a mononuclear three-coordinated derivative, $[CuL(NCMe)]PF_6$, (**1**) where the metal is bonded to both pyrazolyl units and to one molecule of acetonitrile. For silver(I), the complex is dinuclear with

[a]*Departamento de Química Inorgánica, Instituto de Ciencia de Materiales de Aragón Universidad de Zaragoza-C.S.I.C., E-50009, Zaragoza, Spain*
[b]*Departamento de Química e Bioquímica, Faculdade de Ciências da Universidade de Lisboa, 1749-016, Lisboa, Portugal*
[c]*Institut für Anorganische und Analytische Chemie der Technischen Universität, Postfach 3329, D-38023, Braunschweig, Germany*
† Dedicated to Prof. Victor Riera on the occasion of his 70th birthday.
‡ The HTML version of this article has been enhanced with colour images.

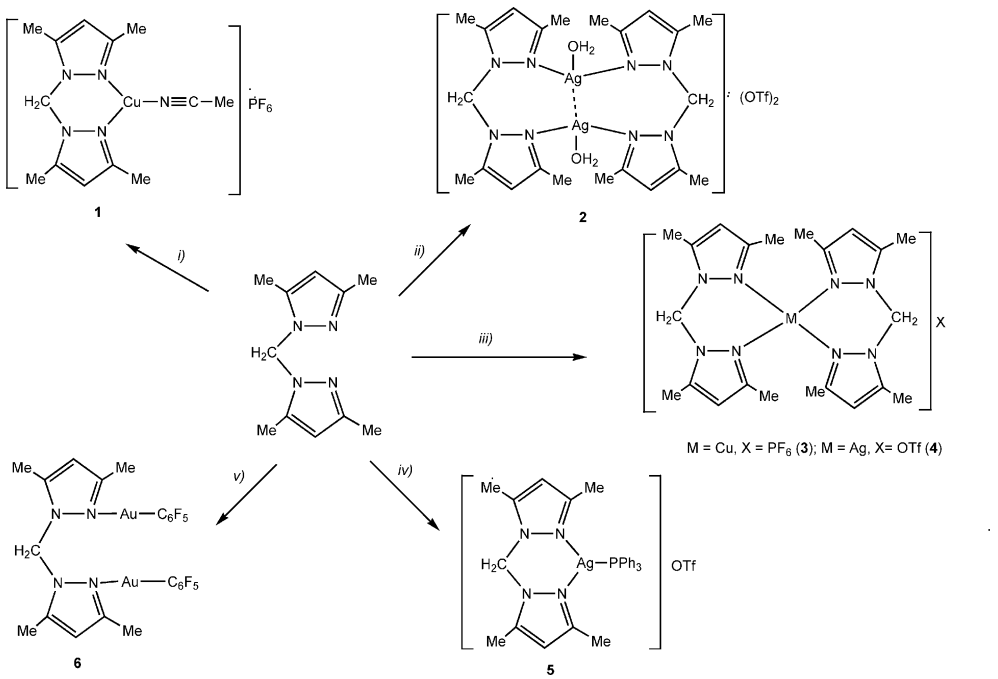

Scheme 1 *Reagents and conditions*: (i) $[Cu(NCMe)_4]PF_6$, (ii) Ag(OTf), (iii) 1/2 $[Cu(NCMe)_4]PF_6$ or Ag(OTf), (iv) $[Ag(OTf)(PPh_3)]$, (v) 2 $[Au(C_6F_5)(tht)]$.

bridging bis(3,5-dimethylpyrazol-1-yl)methane ligands, $[Ag_2(\mu\text{-}L)_2](OTf)_2$ (**2**), and with gold(I) the complex is unstable and could not be isolated. The infrared spectra of these compounds show the characteristic absorption of the pyrazole rings at *ca.* 1556 cm^{-1} that is ever-present in these complexes. For **1**, an intense absorption at 840 cm^{-1} arising from the hexafluorophosphate anion appears. Complex **2** presents the absorptions for the trifluoromethanesulfonate group at 1290, 1241, 1219, 1163 and 1023 cm^{-1}. The ^1H NMR spectra of **1** shows the resonances of the ligand L, two singlets at 2.25 and 2.19 ppm for the inequivalent methyl groups, a singlet for the methylene protons at 5.92 and a singlet for the protons of the pyrazol rings at 5.88 ppm. Additionally, one singlet appears for the methyl protons of the acetonitrile ligand. As we comment below the structure of **2** crystallizes with two water molecules, however in the ^1H NMR spectra these molecules are not observed. The ^{13}C NMR spectra of **1** show the resonances for the carbon atoms of the pyrazole rings, C3, C4, C5 at 142.40, 103.28 and 152.28 ppm, respectively. The methylene carbon appears at 57.39, the methyl carbons at 13.99 and 11.25 and the methyl from the MeCN at 3.26 ppm. In the mass spectrum of **1**, the molecular or the cation molecular peaks are not present; other peaks are present as for example $[CuL_2(NCMe)_2]^+$ at *m*/*z* 553 (49%) and $[CuL(NCMe)_2]^+$ at *m*/*z* 349 (100%) probably arising at association processes. Complex **2** shows similar resonances in the ^1H and ^{13}C NMR spectra for the ligand L, although with different chemical shifts (see Experimental section). The mass spectrum shows the cation molecular peak at *m*/*z* 773 $[Ag_2(OTf)L_2]^+$ (10%).

The structure of the cation of complex **1** is shown in Fig. 1, with a selection of bonds lengths and angles in Table 1. Complex **1** crystallizes in space group $P2_1/m$; the copper atom, the methylene carbon of the bidentate ligand and the acetonitrile atoms (except two methyl hydrogens) lie in a crystallographic plane of symmetry. The Cu(I) centre displays a planar, distorted trigonal geometry, lying just 0.07 Å out of the plane of the three nitrogen atoms; the N–Cu–N angles are 94.80(10)° (within the chelating ligand) and 132.40(5)°. The CuN_4C chelate ring adopts a boat conformation, whereby the four nitrogen atoms are coplanar by symmetry and the atoms Cu and C(1) lie 0.43 and 0.66 Å to the same side of this plane.

Table 1 Bond lengths (Å) and angles (°) for compound **1**

Cu–N(3)	1.874(3)	N(3)–C(7)	1.133(4)
Cu–N(1)	1.9966(19)	C(7)–C(8)	1.460(4)
N(3)–Cu–N(1)	132.40(5)	C(7)–N(3)–Cu	171.6(3)
N(1)[a]–Cu–N(1)	94.80(10)	N(3)–C(7)–C(8)	178.6(4)

Symmetry transformations used to generate equivalent atoms: [a] $x, -y + 1/2, z$.

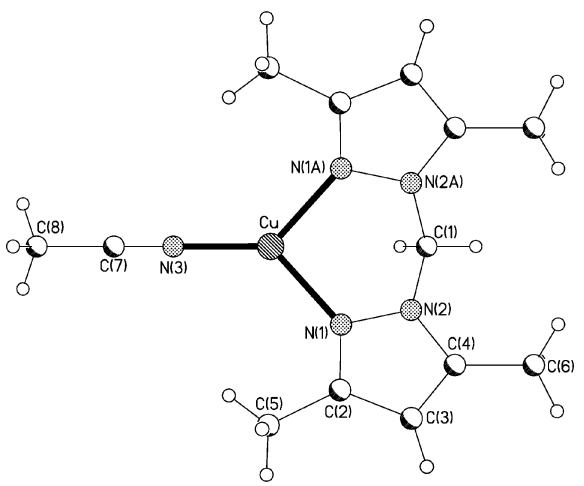

Fig. 1 Structure of the cation of complex **1** in the crystals. The letter "A" in the atom labels indicates symmetry operation $x, 1/2 - y, z$.

The Cu–N bond distances, 1.874(3) [Cu–N(3)] and 1.9966(19) Å [Cu–N(1)], are shorter than those found in the tricoordinated copper(I) derivative $[Cu\{H_2B(3,5\text{-}(CF_3)_2Pz)_2\}(PPh_3)_2]$ (2.057(2) Å)[22] or than most of those found in tetracoordinated copper(I) compounds such as $[Cu(pz_2CPh_2)_2][CuCl_2]$ (Cu–N distances ranging from 2.007(3) to 2.045(3) Å)[23] or $[Cu(H_2CPz_2)(NCMe)_2]ClO_4$ (1.907(8)–2.083(7) Å) and $[Cu(H_2CPz_2)_2]ClO_4$ (2.009(5)–2.120(4) Å).[24] The overall bonding scheme in $[CuL(NCMe)]ClO_4$ is very similar.[21]

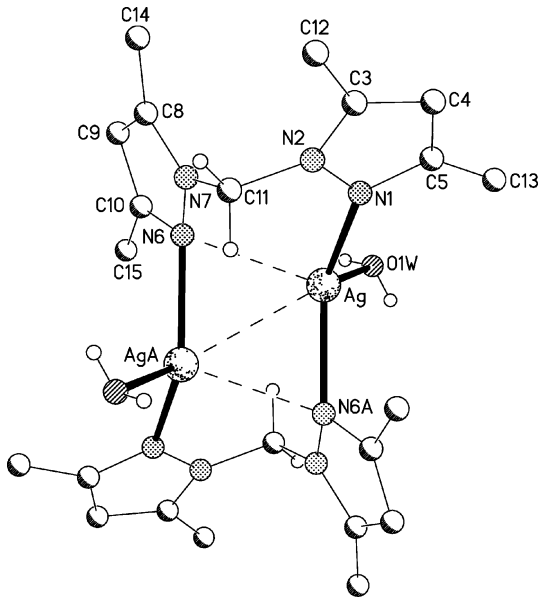

Fig. 2 Structure of the cation of compound **2** in the crystal. "A" in the labels indicates symmetry operation $-x, 2-y, 1-z$.

The structure of compound **2** has been established by an X-ray diffraction study. Selected bond lengths and angles are shown in Table 2. Complex **2** crystallizes in space group $P\bar{1}$ and displays crystallographic inversion symmetry. It crystallizes with two water molecules bonded to the silver atoms; these probably come from crystallization solvent. The structure determination reveals the presence of dimeric species $[Ag_2L_2(H_2O)_2]^{2+}$ linked by bridging L as depicted in Fig. 2. The silver atoms exhibit a highly distorted trigonal coordination with N–Ag–N and N–Ag–O(water) angles in the range 107.00(5)–126.37(5)°, associated with a short Ag···Ag[a] ([a]: $-x, -y+2, -z+1$) contact of 2.9293(3) Å and a short distance Ag–N(6) of 2.6555(12) Å (shown in Fig. 2 as dashes).

Table 2 Selected bond lengths (Å) and angles (°) for compound **2**

Ag–N(1)	2.2201(13)	Ag–N(6)	2.6555(12)
Ag–N(6)[a]	2.2826(13)	Ag–Ag[a]	2.9293(3)
Ag–O(1W)	2.3429(14)		
N(1)–Ag–N(6)[a]	126.37(5)	N(6)–Ag–Ag[a]	47.94(3)
N(1)–Ag–O(1W)	112.18(5)	C(5)–N(1)–Ag	129.54(12)
N(6)[a]–Ag–O(1W)	107.00(5)	N(2)–N(1)–Ag	124.51(10)
N(1)–Ag–N(6)	85.59(4)	C(10)–N(6)–Ag[a]	120.26(10)
N(6)[a]–Ag–N(6)	107.68(3)	N(7)–N(6)–Ag[a]	125.52(9)
O(1W)–Ag–N(6)	117.04(5)	C(10)–N(6)–Ag	125.83(10)
N(1)–Ag–Ag[a]	113.10(4)	N(7)–N(6)–Ag	104.50(8)
N(6)[a]–Ag–Ag[a]	59.74(3)	Ag[a]–N(6)–Ag	72.32(3)
O(1W)–Ag–Ag[a]	129.78(4)		

Symmetry transformations used to generate equivalent atoms: [a] $-x, -y+2, -z+1$.

The Ag–N bond distances, 2.2201(13) Å [Ag–N(1)] and 2.2826(13) Å [Ag–N(6)[a]], are of the same order as those found in tricoordinated silver complexes such as $[Ag_2(L1)_2(H_2O)_2](NO_3)_2$ (L1 = 1,4-bis(2-pyridoxy)benzene),[25] $[Ag_2(L2)_2(H_2O)_2](NO_3)_2$ (L2 = 1,3-bis(2-pyridoxy)benzene)[26] or $[Ag_2(3,5\text{-}(CF_3)_2Pz)_2(2,4,6\text{-collidine})_2]$[27] and compare well with the shortest Ag–N bond distances observed in tetracoordinated silver complexes with bis(pyrazolyl)alkane ligands such as $[Ag\{Me_2C(pz)_2\}_2]ClO_4$,[9] and related systems.[6,28] The Ag–N(6) distance of 2.6555(12) Å suggests the existence of a weak interaction, N(6) being involved in asymmetric bridging between both silver atoms. This type of bridging interaction is reminiscent of that observed in the dinuclear silver complex $[Ag_2(Tp^{MeMe})_2]$ (Tp^{MeMe} = hydrotris(3,5-dimethylpyrazolyl)borate).[29] The Ag–O(water) bond distance, 2.3429(14) Å, is also shorter than those observed in the above mentioned complexes $[Ag_2(L1)_2(H_2O)_2](NO_3)_2$ (L1 = 1,4-bis(2-pyridoxy)benzene)[25] and $[Ag_2(L2)_2(H_2O)_2](NO_3)_2$ (L2 = 1,3-bis(2-pyridoxy)benzene).[26]

In the crystal the ions are associated into chains parallel to the crystallographic *b*-axis *via* short classical hydrogen bonds (Table 3) from the water hydrogens to two triflate oxygens (Fig. 3).

The treatment of the ligand L with $[Cu(NCMe)_4]PF_6$ or Ag(OTf) in a 2 : 1 ratio gives the four-coordinate derivatives $[ML_2]X$ (M = Cu, X = PF_6 (**3**); Ag, X = OTf (**4**)). Their IR spectra present similar IR absorptions except for the PF_6 (**3**) and the OTf (**4**). The ^1H NMR spectra show the absorptions arising from the methyl, methylene and pyrazole H4 protons, with different chemical shifts from the corresponding 1 : 1 complexes. In the mass spectrum of complex **4**, the molecular peak is present at *m*/*z* 773 ($[Ag(OTf)L_2]^+$, 10%) and also the cations $[AgL_2]^+$ at *m*/*z* 515 (56%) and $[AgL]^+$ at *m*/*z* 312 (100%). For compound **3**, only the cation molecular peak is present at *m*/*z* 471 as the most intense peak.

The crystal structure of **3** has been established by X-ray diffraction. The complex crystallizes in the space group $P2_1/c$ with two independent molecules in the asymmetric unit. Selected bond lengths and angles are collected in Table 4. The cation of one of the independent molecules is shown in Fig. 4. The Cu(I) atoms display a distorted tetrahedral geometry with N–Cu–N angles ranging from 95.43(9)° [N(1)–Cu(1)–N(4)] and 95.68(10)° [N(12)–Cu(2)–N(9)] to 134.61(9)° [N(1)–Cu(1)–N(8)] and 134.22(9)° [N(12)–Cu(2)–N(16)]. Cu–N bond distances (range from 1.982 to 2.099 Å) compare well with those observed in other tetracoordinated copper(I) complexes.[10,11] The six-membered CuN_4C rings adopt a boat conformation, with the atoms Cu(1) and C(6) lying −0.26 and −0.97 Å, and Cu(1) and C(17), −0.29 and −0.69 Å to the same side of the N4 planes.

Table 3 Hydrogen bonds (Å and °) for compound **2**

D–H···A	*d*(D–H)	*d*(H···A)	*d*(D···A)	∠(DHA)
O(1W)–H(01W)···O(2)[a]	0.74(2)	2.03(2)	2.764(2)	170(3)
O(1W)–H(02W)···O(3)	0.75(2)	2.06(2)	2.810(2)	178(3)
C(14)–H(14B)···O(1W)[b]	0.98	2.60	3.405(2)	139.5
C(4)–H(4)···O(1)[c]	0.95	2.50	3.387(2)	155.0

Symmetry transformations used to generate equivalent atoms: [a] $-x, -y+1, -z+1$. [b] $-x+1, -y+2, -z+1$. [c] $x, y, z+1$

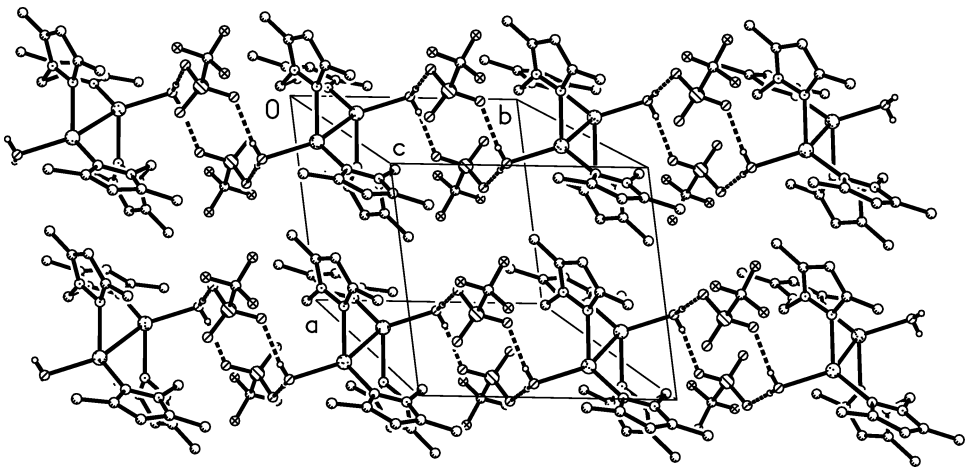

Fig. 3 Supramolecular structure *via* hydrogen bonding in complex **2**.

Table 4 Selected bond lengths (Å) and angles (°) for complex **3**

Cu(1)–N(1)	1.986(3)	Cu(2)–N(12)	1.982(3)
Cu(1)–N(8)	1.995(3)	Cu(2)–N(16)	1.993(3)
Cu(1)–N(5)	2.073(3)	Cu(2)–N(13)	2.067(3)
Cu(1)–N(4)	2.099(2)	Cu(2)–N(9)	2.097(2)
N(1)–N(2)	1.376(3)	N(9)–N(10)	1.354(3)
N(3)–N(4)	1.364(3)	N(11)–N(12)	1.369(3)
N(5)–N(6)	1.367(3)	N(13)–N(14)	1.359(3)
N(7)–N(8)	1.374(3)	N(15)–N(16)	1.363(3)
N(1)–Cu(1)–N(8)	134.61(9)	N(12)–Cu(2)–N(16)	134.22(9)
N(1)–Cu(1)–N(5)	111.23(11)	N(12)–Cu(2)–N(13)	111.33(11)
N(8)–Cu(1)–N(5)	95.80(10)	N(16)–Cu(2)–N(13)	96.01(10)
N(1)–Cu(1)–N(4)	95.43(9)	N(12)–Cu(2)–N(9)	95.68(10)
N(8)–Cu(1)–N(4)	110.52(10)	N(16)–Cu(2)–N(9)	110.73(11)
N(5)–Cu(1)–N(4)	107.88(9)	N(13)–Cu(2)–N(9)	107.36(9)

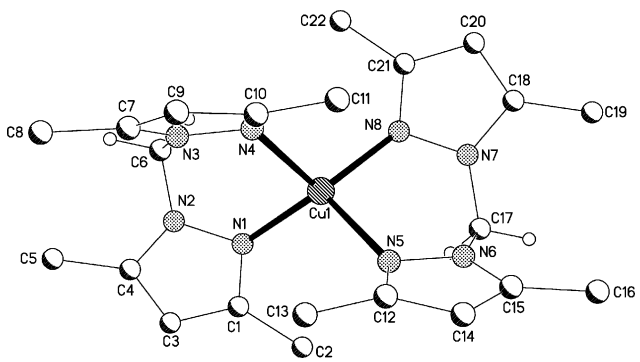

Fig. 4 Structure of the cation of complex **3**.

The structure of complex **4** is shown in Fig. 5. Selected bond lengths and angles are collected in Table 5. The silver centre displays a highly distorted tetrahedral geometry; angles around Ag range from 85.40(5)° [N(5)–Ag(1)–N(8)] to 144.73(5)° [N(5)–Ag(1)–N(1)]. The angle between the two mean planes defined by N(1), Ag(1) and N(4) and N(5), Ag(1) and N(8) is 103.4° (a interplanar angle of 90° is expected for a perfect tetrahedron). The AgN_4C chelate rings adopt boat conformations, with the Ag(1) and C(6) atoms lying −0.37 and −0.69 Å, and the Ag(1) and C(17) lying 0.57 and 0.70 Å to the same side of the N4 planes. The second molecule presents a similar boat conformation.

Table 5 Selected bond lengths (Å) and angles (°) for complex **4**

Ag(1)–N(5)	2.2341(13)	Ag(1)–N(1)	2.3146(13)
Ag(1)–N(4)	2.2906(13)	Ag(1)–N(8)	2.4064(14)
N(5)–Ag(1)–N(4)	120.41(5)	N(5)–Ag(1)–N(8)	85.40(5)
N(5)–Ag(1)–N(1)	144.73(5)	N(4)–Ag(1)–N(8)	115.42(5)
N(4)–Ag(1)–N(1)	86.80(5)	N(1)–Ag(1)–N(8)	103.66(5)

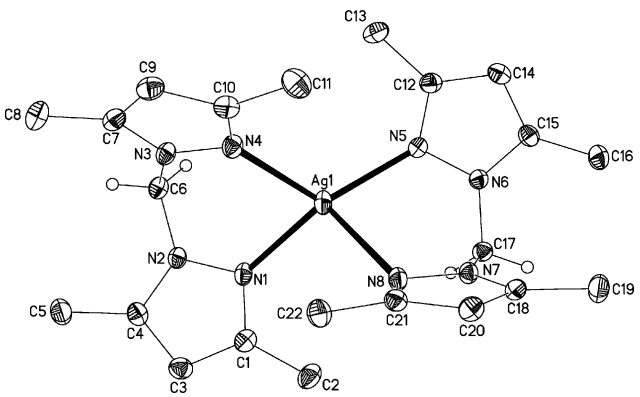

Fig. 5 Structure of the cation of complex **4**.

The Ag–N bond distances, from 2.2341(13) to 2.4064(14) Å, compare well with those found in the related complexes $[Ag\{Me_2C(pz)_2\}_2]ClO_4$[9] (range from 2.247(4) to 2.432(4) Å), or in other tetrahedral silver complexes with bis(pyrazolyl)alkane ligands (range from 2.243(4) to 2.5092(19) Å).[6,28] Additional C–H···O(anion) hydrogen bonds present in complex **4** are collected in Table 6.

Table 6 Hydrogen bonds for complex **4** (Å and °)

D–H···A	*d*(D–H)	*d*(H···A)	*d*(D···A)	∠(DHA)
C(11)–H(11B)···O(3)[a]	0.98	2.50	3.454(2)	164.5
C(5)–H(5C)···O(3)[b]	0.98	2.54	3.459(2)	156.6
C(6)–H(6A)···O(3)[b]	0.99	2.43	3.415(2)	172.4
C(19)–H(19B)···O(1)[c]	0.98	2.52	3.410(2)	151.0
C(16)–H(16B)···O(1)[d]	0.98	2.45	3.409(2)	167.3

Symmetry transformations used to generate equivalent atoms: [a] $x, -y + 1/2, z + 1/2$. [b] $-x + 1, -y + 1, -z + 1$. [c] $-x + 1, -y, -z + 1$. [d] $x - 1, y, z$.

The reaction of L with [Ag(OTf)(PPh_3)] in 1 : 1 or 1 : 2 ratio affords the same derivative [AgL(PPh_3)]OTf (**5**). A similar reaction with the gold(I) precursor [Au(OTf)(PPh_3)] and the ligand gave a mixture of complexes. The IR spectrum of **5** shows the bands of the triflate ligand at 1280, 1251, 1224, 1156 and 1030 cm^{-1}, which are characteristic of coordinated triflate. The ^1H NMR spectrum shows the typical resonances for the ligand and the phenyl protons and the $^{31}P\{^1H\}$ NMR presents a broad signal at room temperature that splits into two doublets at low temperature because of the coupling of the phosphorus atoms with the two silver ^{109}Ag and ^{107}Ag nuclei. The mass spectrum shows the cation molecular peak [AgL(PPh_3)]$^+$ at m/z 573 as the most intense. Other fragments are [AgL]$^+$ (85%) and [Ag(PPh_3)]$^+$ (50%).

Finally, we carried out the reaction of the ligand L with two equivalents of [Au(C_6F_5)(tht)] and obtained a pure gold(I) derivative, [$Au_2(C_6F_5)_2$(μ-L)] (**6**). The IR spectrum of **6** presents bands at 1507, 957 and 807 cm^{-1} from the pentafluorophenyl groups bonded to gold(I). In the ^{19}F NMR spectrum three resonances for the pentaflurophenyl rings appear and are two multiplets for the *ortho* and *meta* fluorine and a triplet for the *para* fluorine in the ratio 2 : 2 : 1, respectively. The ^1H NMR spectrum shows the characteristic resonances for the ligand bis(3,5-dimethylpyrazol-1-yl)methane.

Luminescence studies

Complexes **1–6** are luminescent in the solid state at 77 K. All of them display an emission that occurs in a modest range of the spectrum, with local maxima spanning approximately 90 nm (see Table 7). An emission at similar energies is also observed in the spectrum of the free ligand, at 459 nm. Nevertheless the coordination of the ligand increases the intensity of the emission. In compound **6** the band displays three maxima at 431, 448 and 460 nm.

Similar emissions have been described for complexes with N-aryl ligands, such as 2-(aminomethyl)pyridine, in this case, the emissions increase their intensities upon coordination of the counteranion, and the formation of polymeric structures.[30] The origin has been attributed to intraligand transitions, with contribution of charge transfer character. The emissions of complexes with 2-(diphenylphosphino)aniline[31] or of pyrazolato–gold(I) complexes were observed in the same range,[32] and were assigned mainly to ligand to metal charge transfer processes.

In addition to the commented emission, compound **5** also displays an emission at lower energy (504 nm) and the emission spectrum of compound **4** shows a shoulder in the band previously commented. For compound **4** upon excitation at 300 nm the shoulder is not observed (see Fig. 6), whereas in the case of compound **5** (Fig. 7) the band at 504 is not observed upon excitation at 300 nm. In both cases, the intensity of the band at higher energies decreases upon excitation at lower energies. These observations could enhance the idea of an important contribution of ligand to metal charge transfer in the nature of the emissions.

Table 7 Luminescence spectral data for the ligand and compounds **1–6** in the solid state at 77 K

Compound	Emission, λ_{max}[a]	Excitation, λ_{max}[a]
L	459	363
1	420	300/330
2	402/434	315
3	489	306
4	410/shoulder 490	284/350
5	406/508	300/330
6	431/448/460	305/370

[a] λ_{max} in nm.

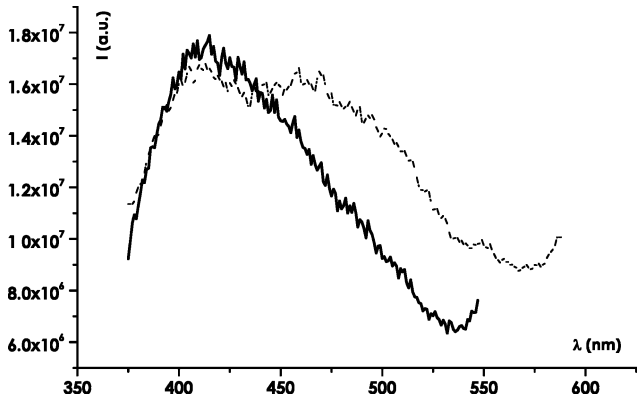

Fig. 6 Emission spectrum of **4** with maximum of excitation at $\lambda = 305$ nm (solid line) and 335 nm (dashed line).

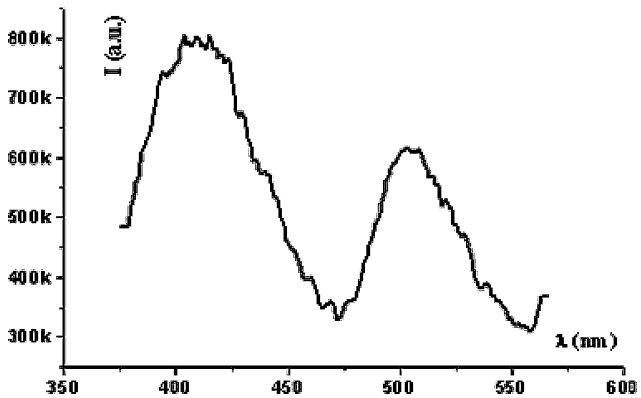

Fig. 7 Emission spectrum of **5** with maximun of excitation at $\lambda = 340$ nm.

DFT calculations

DFT calculations[33] (ADF program[34]) were performed in models of some Ag(I) and Cu(I) complexes, in order to understand their structural preferences. The methyl groups of the bis(3,5-dimethylpyrazol-1-yl)methane (**L**) ligand were always replaced by hydrogen atoms, to give bis(pyrazol-1-yl)methane (**L′**). The most interesting structure is that of the Ag(I) complex [Ag_2(μ-$L)_2(H_2O)_2$]$(OTf)_2$ **2**, where silver achieves an unusual coordination environment. Besides the coordination to two nitrogen atoms of L, there is a short Ag···Ag contact, a relatively short Ag–O distance to coordinated water and a weak Ag···N bond, as described above. Why does silver adopt such a structure? The full optimization (see Computational details section for more) without symmetry constraints of the dication [Ag_2(μ-$L')_2(H_2O)_2$]$^{2+}$ led to significant changes in the conformation of the rings and the overall geometry, as shown in Fig. 8 (left, top). A comparison with the X-ray structure (Fig. 8, right) reveals that the Ag···Ag and Ag–O distances increased to 3.079 and 2.811 Å, respectively,

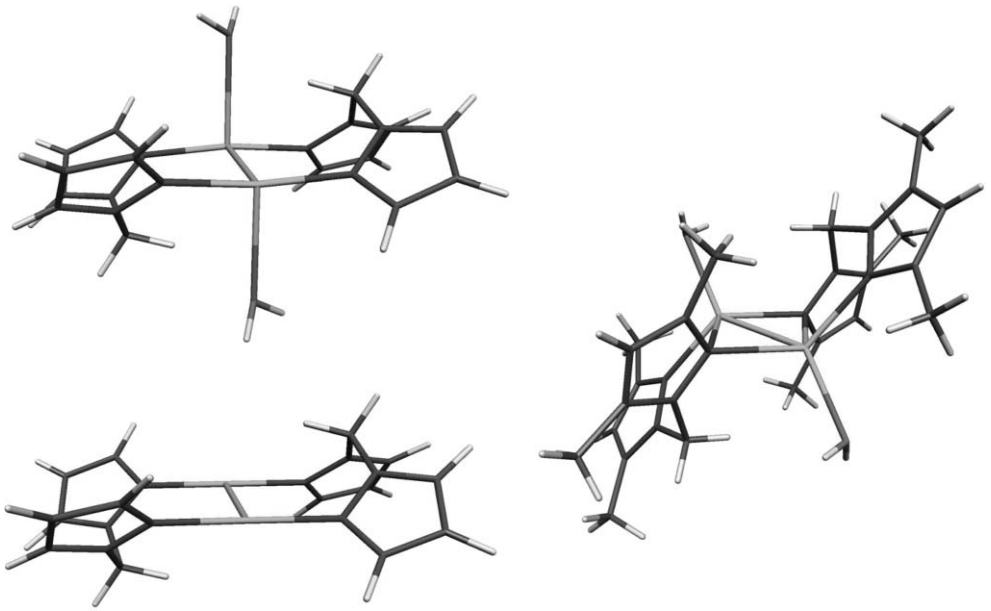

Fig. 8 ADF optimized structure of $[Ag_2(\mu\text{-}L')_2(H_2O)_2]^{2+}$ (top left) and $[Ag_2(\mu\text{-}L')_2]^{2+}$ (bottom left) compared with the observed structure (right).

while the long Ag–N bond has disappeared. The Ag–N bonds (2.109, 2.110 Å) became significantly shorter than the initial 2.2201(13) and 2.2826(13) Å. The 12-membered ring adopts a chair conformation, with a N–Ag–N···N–Ag–N plane, instead of a N–Ag–N–Ag plane.

These results are not expected, as DFT calculations are known for their very good reproduction of ground-state structures. The structure was optimized again, after removing the water molecules. While the shape of the dication is retained, despite the loss of water (Fig. 8, bottom left), the Ag–N bonds become shorter (2.084–2.088 Å) and the Ag···Ag distance lengthens slightly to 3.117 Å. The binding energy of each water molecule to the silver fragment $[Ag_2(\mu\text{-}L')_2]^{2+}$ was calculated as 9.6 kcal mol^{-1}.

Interestingly, there is a very similar complex structurally characterized in the literature, with pyrazole replaced by imidazole, $[Ag_2(\mu\text{-}L^*)_2]^{2+}$ [L* = bis(imidazol-2-yl)methane)], shown in Fig. 9.[35] The Ag···Ag distance is 3.261 and the Ag–N bonds 2.095 and 2.096 Å. These values compare very well with the calculated geometry of $[Ag_2(\mu\text{-}L')_2]^{2+}$ and there is no problem of reproducing the Ag···Ag bond length.

For comparison, a full geometry optimization without symmetry constraints was also carried out for the $[AgL'_2]^+$ model of the cation of complex **4**. In this complex, the calculated Ag–N distances range from 2.245 to 2.434 Å, reproducing very well the observed distances, 2.2341(15)–2.4064(14) Å, and the other parameters are also similar. Since distances are not always the best indicators of bond strength, Mayer indices[36] were also calculated and are shown in Table 8. It is clear that the calculated $[Ag(L')_2]^+$ cation is very similar to the parent compound **4**, both when analyzing bond lengths and bond strengths (MIs), despite the use of a model for the ligand. The experimental asymmetry between Ag–N bonds is also maintained.

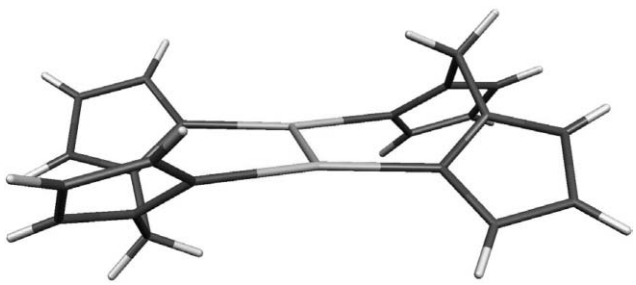

Fig. 9 Experimental structure of $[Ag_2(\mu\text{-}L^*)_2]^{2+}$ [L* = bis(imidazol-2-yl)methane)].[35]

Table 8 Mayer indices and distances (Å, parenthesis) for the Ag–N, Ag–O, and Ag–Ag bonds in complexes **2** and **4** and their models

	Ag–N1[a]	Ag–N6A[a]	Ag–N6[a]	Ag–Ag	Ag–O
$[Ag_2(\mu\text{-}L)_2(H_2O)_2]^{2+}$, **2**	0.407 (2.220)	0.377 (2.283)	0.150 (2.655)	0.176 (2.929)	0.211 (2.343)
$[Ag_2(\mu\text{-}L')_2(H_2O)_2]^{2+}$	0.462 (2.109)	0.451 (2.109)		0.216 (3.078)	0.098 (2.811)
$[Ag_2(\mu\text{-}L')_2]^{2+}$	0.476 (2.084)	0.474 (2.088)		0.201 (3.117)	—
	Ag–N	Ag–N	Ag–N	Ag–N	
$[Ag(L)_2]^+$, **4**	0.373 (2.233)	0.331 (2.291)	0.329 (2.315)	0.272 (2.406)	
$[Ag(L')_2]^+$	0.362 (2.245)	0.330 (2.303)	0.306 (2.335)	0.259 (2.434)	—

[a] See Fig. 2 for numbering scheme.

This conclusion led us to search for an explanation of the unexpected behavior of the model of complex **2**. A detailed look at the packing of the complex indicates that the dication with two water molecules are intimately involved in a crystal network. The water molecules participate in hydrogen bonds with the triflate anions, which act as bridges between $[Ag_2(\mu\text{-}L')_2(H_2O)_2]^{2+}$ units, giving rise to a 3-D network. This seems to be one rare example of a structure where the intermolecular interactions force the covalent bonds to change. Besides the Ag···Ag distance, which barely changes when water is removed in our calculation, Ag(I) in **2** makes three Ag–N bonds: two very strong ones and a weaker one. No such strong bonds are detected in complex **4** or its model. Interestingly, the Ag–N bonds are even stronger in the model of **2**, $[Ag_2(\mu\text{-}L')_2(H_2O)_2]^{2+}$, but the third bond has been lost. As long as water molecules are available to provide a driving force for the formation of strong hydrogen bonds, this structure becomes very favourable. Notice that with Cu(I) the result of the 1 : 1 reaction is complex **1**, a mononuclear species with one nitrile. In the presence of water (less care in handling inert conditions), no product was isolated. Indeed, Cu(I) is oxidized to Cu(II) in such conditions.

There are examples in the literature of similar arrangements, where two silver atoms are linked by a bridging nitrogen ligand, and each silver atom further binds one water molecule. The Ag···Ag distance varies widely. For instance, in the most comparable system, $[Ag_2(L1)_2(H_2O)_2](NO_3)_2$ (L1 = 1,4-bis(2-pyridoxy)benzene),[25] the silver atoms are 9.405 Å apart, each one coordinates one water molecule (Ag–O distance 2.485, 2.486 Å) and the water molecules are involved in a 3-D hydrogen bond network with the nitrate counter ion. The only difference is the Ag···Ag contact. There is no argentophilicity in this system. In other related cases, when water is absent, silver coordinates one (or two) oxygen atoms of the counterion, giving rise to similar motifs, but with a different packing.

For instance, in complex $[Ag_2(L3)_2](NO_3)_2$[37] (L3 = 1,4-bis(2-pyridylsulfanylmethyl)benzene), there is also no Ag···Ag interaction (the Ag···Ag distance is 12.196 Å) and each Ag is coordinated to two oxygen atoms of the nitrate (2.591 and 2.638 Å), being also involved in weak interactions with the two close S atoms (2.166 and 2.591 Å). The complex $[Ag_2(L4)_2](ClO_4)_2$[35] (L4 = bis(1-benzylimidazol-2-yl)methanol) exhibits a close contact (3.018 Å) and the frame of the molecule is quite distorted, though not in the same way as complex **2**. Each silver atom is bound to two nitrogen atoms (2.112–2.141 Å) of the bridging ligands, one oxygen of the ClO_4^- anion (3.012 or 3.211 Å), and there is a weak Ag···Ag interaction.

Conclusions

Our results show that Ag(I) reacts with bidentate nitrogen ligands, such as bis(3,5-dimethylpyrazol-1-yl)methane to form binuclear species (complex **2**), where the ligands act as bridges, one water molecule binds each Ag and there is a short Ag···Ag contact. An analogous reaction with Cu(I) gives a mononuclear species. In 1 : 2 ratio, mononuclear complexes ML_2 are formed for Cu(I) and Ag(I).

The structure of the dication $[Ag_2(\mu\text{-}L)_2(H_2O)_2]^{2+}$ could not be reproduced by DFT calculations, though the optimized geometry is very similar to that of a related Ag(I) complex without coordinated water. We concluded that coordination of H_2O to Ag in the binuclear complex allows the formation of a hydrogen bond network, releasing enough energy to allow distortion of the Ag_2 framework.

The ligand is weakly emissive (459 nm) at 77 K and the luminescence increases upon coordination to the metal centres. The complexes show maximum energy emissions between 410 and 508 nm. The origin of the emissions could be assigned to intraligand and metal charge transfer transitions.

Experimental

The starting materials $[Cu(NCMe)_4]PF_6$,[38] $[Au(C_6F_5)(tht)]$ (tht = tetrahydrothiophene),[39] $[Ag(OTf)(PPh_3)]$,[40] and the ligand bis(3,5-dimethylpyrazol-1-yl)methane[41] were prepared by published procedures. Syntheses of the copper complexes were carried out under argon atmosphere. Solvents were dried using common procedures. All other chemicals used were commercially available and used without further purification. NMR spectra were recorded on a Varian Unity 300 spectrometer and a Bruker ARX 300 or Bruker Avance 400 spectrometers in $CDCl_3$ or CD_2Cl_2. Chemical shifts are cited relative to $SiMe_4$ (^1H, ^{13}C, external), $CFCl_3$ (^{19}F, external) and 85% H_3PO_4 (^{31}P, external). Infrared spectra were recorded in the range 4000–350 cm^{-1} on a Perkin-Elmer Spectrum One spectrophotometer using Nujol mulls between polyethylene sheets or KBr pellets. C, H, N and S analyses were carried out with a Perkin-Elmer 2400 microanalyzer. Mass spectra were recorder on a VG Autospec, with the LSIMS technique, using nitrobenzyl alcohol as matrix. Steady-state photoluminescence spectra were recorded with a Jobin-Yvon Horiba Fluorolog FL-3-11 spectrometer using band pathways of 3 nm for both excitation and emission.

Synthesis of $[CuL(NCMe)]PF_6$ (1)

To a solution (ethanol, 40 ml) of $[Cu(NCMe)_4]PF_6$ (0.3 mmol, 0.112 g) in ethanol was added **L** (0.3 mmol, 0.061 g). After 10 minutes, a white precipitate was formed. The stirring was continued for 3 h. The white precipitate (complex **1**) was filtered off, washed with 3 × 10 ml of diethyl ether and dried under vacuum. Yield: 75%. Anal. Calc. for $C_{13}H_{19}N_5CuPF_6$: C, 34.40; H, 4.22; N, 15.43%. Found: C, 34.38; H, 4.27; N, 15.04%. ^1H NMR, CD_2Cl_2, δ: 5.92 (s, CH_2), 5.88 (s, H4), 2.31 (s, CH_3), 2.25 (s, $NCCH_3$), 2.19 (s, CH_3) ppm. ^{13}C NMR, CD_2Cl_2, δ: 152.28 (C5), 142.40 (C3), 107.28 (C4), 57.39 (CH_2), 13.99 (CH_3), 11.25 (CH_3), 3.26 (CH_3CN) ppm. FAB-MS (m/z): 553 ($[CuL_2(NCCH_3)_2]^+$, 49%), 471 ($[CuL_2]^+$, 75%), 349 ($[CuL(NCMe)_2]^+$, 100%). The crystals were obtained from dichloromethane–hexane.

Synthesis of $[Ag(\mu\text{-}L)]_2(OTf)_2$ (2)

To a dichloromethane solution (20 mL) of L (L = bis(3,5-dimethylpyrazol-1-yl)methane) (0.5 mmol, 0.102 g) was added Ag(OTf) (0.5 mmol, 0.128 g). The reaction mixture was stirred for 1 h, concentrated to *ca.* 5 mL, and addition of diethyl ether (15 mL) led to complex **2** as a white solid. Yield: 75%. Anal. Calc. for $C_{24}H_{32}N_8Ag_2S_2O_6F_6$ (%): C, 31.25; H, 3.50; N, 12.15; S, 6.95. Found: C, 31.43; H, 3.27; N, 12.23; S, 6.79. ^1H NMR, $CDCl_3$, δ: 6.44 (s, CH_2), 6.03 (s, H4), 2.36 (s, CH_3), 2.22 (s, CH_3) ppm. ^{13}C NMR, $CDCl_3$, δ: 152.42 (C5), 142.65 (C3), 108.17 (C4),

60.15 (CH_2), 14.53 (CH_3), 11.51 (CH_3) ppm. FAB-MS (*m*/*z*): 773 ($[AgL_2(OTf)]^+$, 10%), 515 ($[AgL_2]^+$, 18%), 312 ($[AgL]^+$, 100%). The crystals were obtained from dichloromethane–hexane.

Synthesis of $[CuL_2]PF_6$ (3)

To a solution (ethanol, 70 ml) of $[Cu(NCMe)_4]PF_6$ (0.3 mmol, 0.112 g) was added L (0.6 mmol, 0.122 g). After 10 min, a white precipitate was formed. The stirring was continued for 5 h. The white precipitate (complex **3**) was filtered off, washed with 3 × 10 ml of diethyl ether and dried under vacuum. Yield: 77%. Anal. Calc. for $C_{22}H_{32}N_8CuPF_6$: C 42.82, H 5.23, N 18.16%. Found: C, 42.69; H, 5.34; N, 18.32%. ^{1}H NMR, CD_2Cl_2, δ: 6.06 (s, CH_2), 5.86 (s, H4), 2.36 (s, CH_3), 1.75 (s, CH_3) ppm. ^{13}C NMR, CD_2Cl_2, δ: 150.38 (C5), 140.50 (C3), 106.86 (C4), 57.59 (CH_2), 13.40 (CH_3), 11.20 (CH_3) ppm. FAB-MS (*m*/*z*): 471 ($[CuL_2]^+$, 100%). The crystals were obtained from dichloromethane–hexane.

Synthesis of $[AgL_2](OTf)$ (4)

To a dichloromethane solution (20 mL) of L (0.5 mmol, 0.102 g) was added Ag(OTf) (0.25 mmol, 0.064 g) and the mixture stirred for 1 h. The solution was concentrated to *ca.* 5 mL and addition of hexane (15 mL) gave complex **4** as a white solid. Yield: 73%. Anal. Calc. for $C_{23}H_{32}N_8AgSO_3F_3$: C, 41.51; H, 4.85; N, 16.84; S, 4.82. Found: C, 41.20; H, 4.84; N, 16.54; S, 4.99. ^{1}H NMR, CD_2Cl_2, δ: 6.24 (s, CH_2), 5.88 (s, H4), 2.47 (s, CH_3), 2.00 (s, CH_3) ppm. ^{13}C NMR, CD_2Cl_2, δ: 150.19 (C5), 141.11 (C3), 106.58 (C4), 58.61 (CH_2), 13.76 (CH_3), 11.16 (CH_3) ppm. FAB-MS (*m*/*z*): 773 ($[AgL_2(OTf)]^+$, 10%), 515 ($[AgL_2]^+$, 56%), 312 ($[AgL]^+$, 100%). The crystals were obtained from dichloromethane–hexane.

Synthesis of $[AgL(PPh_3)](OTf)$ (5)

To a solution of $[Ag(OTf)(PPh_3)]$ (0.3 mmol, 0.156 g) in dichloromethane (20 mL) was added L (0.3 mmol, 0.061 g) and the mixture stirred for 1 h. Concentration of the solution to *ca.* 5 mL and addition of diethyl ether gave complex **5** as a white solid. Yield: 76%. Anal. Calc. for $C_{30}H_{31}N_4AgPSO_3F_3$ (%): C, 49.80; H, 4.32; N, 7.74; S, 4.43. Found: C, 49.52; H, 4.38; N, 7.60; S, 4.21. ^{1}H NMR, $CDCl_3$, δ: 7.55–7.45 (m, 15 H, Ph), 6.43 (s, CH_2), 5.88 (s, H4), 2.48 (s, CH_3), 1.95 (s, CH_3) ppm. ^{13}C NMR, $CDCl_3$, δ: 150.62 (C5), 142.13 (C3), 133.95 (C_o), 133.79 (C_o), 131.23 (C_p, Ph), 130.10 (d, C_{ipso}, *J*(PC) 38.20 Hz), 129.39 (C_m), 129.28 (C_m), 106.82 (C4), 58.45 (CH_2), 14.14 (CH_3), 11.17 (CH_3) ppm. ^{31}P{^{1}H} NMR, $CDCl_3$ (−50 °C), δ: 16.54 [2d, br, *J*(^{107}AgP) 680 Hz, *J*(^{109}AgP) 786 Hz] ppm. FAB-MS (*m*/*z*): 573 ($[AgL(PPh_3)]^+$, 100%), 369 ($[Ag(PPh_3)]^+$, 50%), 311 ($[AgL]^+$, 85%).

Synthesis of $[\{Au(C_6F_5)\}_2(\mu\text{-}L)]$ (6)

To a dichloromethane solution (20 mL) of $[Au(C_6F_5)(tht)]$ (tht = tetrahydrothiophene; 0.4 mmol, 0.181 g) was added L (0.2 mmol, 0.041 g). The reaction mixture was stirred for 1 h, concentrated to *ca.* 5 mL, and addition of hexane (15 mL) led to complex **6** as a white solid. Yield: 60%. Anal. Calc. for $C_{23}H_{16}N_4Au_2F_{10}$: C, 29.63; H, 1.73; N, 6.01. Found: C, 29.90; H, 2.03; N, 6.30. ^{1}H NMR, CD_3Cl, δ: 6.98 (s, CH_2), 6.08 (s, H4), 2.43 (s, CH_3), 2.37 (s, CH_3). ^{13}C NMR, $CDCl_3$, δ: 152.49 (C5), 144.43 (C3), 109.65 (C4),

Table 9 X-Ray crystal data for complexes **1**, **2**, **3** and **4**

Compound	**1**	**2**	**3** CH_2Cl_2	**4**
Formula	$C_{13}H_{19}CuF_6N_5P$	$C_{24}H_{36}Ag_2F_6N_8O_8S_2$	$C_{23}H_{34}Cl_2CuF_6N_8P$	$C_{23}H_{32}AgF_3N_8O_3S$
M_r	453.84	958.46	701.99	665.50
Habit	Colourless tablet	Colourless prism	Colourless needle	Colourless prism
Crystal size/mm	0.30 × 0.30 × 0.08	0.37 × 0.19 × 0.10	0.27 × 0.12 × 0.09	0.42 × 0.32 × 0.20
Crystal system	Monoclinic	Triclinic	Monoclinic	Monoclinic
Space group	$P2_1/m$	$P\bar{1}$	$P2_1/c$	$P2_1/c$
a/Å	7.5202(8)	9.0683(8)	14.5580(18)	13.8993(6)
b/Å	13.0771(14)	9.9695(8)	14.3493(13)	15.4860(6)
c/Å	9.2673(11)	11.7296(10)	28.765(3)	14.2529(6)
α/°	90	65.370(3)	90	90
β/°	95.981(4)	70.331(3)	90.219(8)	112.878(6)
γ/°	90	81.970(3)	90	90
V/Å^3	906.41(17)	907.71(13)	6008.9(11)	2826.5(2)
Z	2	1	8	4
D_c/Mg m^{-3}	1.663	1.753	1.552	1.564
μ/mm^{-1}	1.359	1.279	1.025	0.847
F(000)	460	480	2880	1360
T/°C	−120	−130	−173	−173
$2\theta_{max}$/°	57	60	64	64
No. of refl.:				
measured	13077	19742	48286	24203
independent	2438	5295	17786	8881
Transmissions	0.69–0.90	0.81–0.96	0.69–0.91	0.70–0.85
R_{int}	0.034	0.019	0.091	0.016
Parameters	145	238	828	360
Restraints	21	1	0	0
$wR(F^2$, all refl.)	0.101	0.064	0.079	0.078
$R(F > 4\sigma(F))$	0.037	0.024	0.050	0.028
S	1.048	1.032	0.709	1.117
$\Delta\rho_{max}$/e Å^{-3}	0.55	0.711	0.356	1.108

61.38 (CH_2), 14.24 (CH_3), 12.88 (CH_3) ppm. ^{19}F NMR, $CDCl_3$, δ: −117.15 (m, 4 F, *o*-F), −159.81 (t, 2 F, *p*-F, $J(F_p,F_m) = 20.05$ Hz), −163.62 (m, 4 F, *m*-F) ppm. FAB-MS (*m*/*z*): 932 ($[Au_2(C_6F_5)_2L]^+$, 35%), 765 ($[Au_2(C_6F_5)L]^+$, 70%), 568 ($[Au(C_6F_5)L]^+$, 60%), 401 ($[AuL]^+$, 100%).

Crystal structure determinations

Data were registered on a Bruker Smart 1000 CCD (**1**, **2**) or Oxford Diffraction Xcalibur (**3**, **4**) diffractometers. The crystals were mounted in inert oil on glass fibres and transferred to the cold gas stream of the diffractometer. Data were collected using monochromated Mo-Kα radiation ($\lambda = 0.71073$) in ω (**3**, **4**) or ω- and φ-scans. Absorption corrections based on multiple scans were applied with the program SADABS. The structures were solved by direct methods and refined on F^2 using the program SHELXL-97.[42] All non-hydrogen atoms were refined anisotropically. Further crystal data are given in Table 9. *Special features of refinement*: The anion of compound (**1**) is disordered over two positions with common axial F sites. Water H of compound (**2**) were refined freely, but with O–H distances restrained to be equal. Crystals of complex **3** slowly lose solvent even at low temperature and for that reason the data are not good. The structure was refined in the monoclinic space group $P2_1/c$ but can be also solved and refined in the orthorhombic space group *Pbca*, however the β angle of 90.2° is too far away from 90°. Furthermore the R_{int}, R_{sigma} and the final *R* values are slightly better for the monoclinic space group.

CCDC reference numbers 604024–604027.

For crystallographic data in CIF or other electronic format see DOI: 10.1039/b605034d

Computational details

Density functional calculations[33] were carried out with the Amsterdam Density Functional program (ADF2005).[34] Gradient corrected geometry optimizations[43] without any symmetry constraints were performed using the Local Density Approximation of the correlation energy (Vosko, Wilk and Nusair's),[44] and the Generalized Gradient Approximation (Perdew–Wang[45] exchange and correlation corrections). A triple-ζ Slater-type orbital (STO) basis set augmented by two polarization functions was used for all atoms. A frozen core approximation was used to treat the core electrons: (1s) for C, O and N; ([1–3]s [2–3]p 3d) for Ag. Relativistic effects were treated with the ZORA approximation.[46] Mayer indices[36] were calculated and used as bond strength indicators. Three-dimensional representations of molecules were obtained with Molekel.[47]

Acknowledgements

We thank the Ministerio de Educación y Ciencia (BQU2004-05495-C02-01) for financial support. We thank the Acción Integrada HP20030147 and Acção Integrada E-31/04. P. J. C. acknowledges FCT for grant (SFRH/BD/10535/2002) and S. Quintal for grant (SFRH/BPD/11463/2002).

References

1 S. Trofimenko, *J. Am. Chem. Soc.*, 1970, **70**, 5118.
2 S. Trofimenko, *Prog. Inorg. Chem.*, 1986, **34**, 115.
3 P. K. Byers, A. J. Canty and R. T. Honeyman, *Adv. Organomet. Chem.*, 1992, **34**, 1.
4 L. D. Field, B. A. Messerle, L. Soler, I. E. Buys and T. W. Hambley, *J. Chem. Soc., Dalton Trans.*, 2001, 1959.
5 G. Sánchez, J. L. Serrano, J. Pérez, M. C. Ramírez de Arellano, G. López and E. Molins, *Inorg. Chim. Acta*, 1999, **295**, 136.
6 D. L. Reger, J. R. Gardinier and M. D. Smith, *Inorg. Chem.*, 2004, **43**, 3825.
7 D. L. Reger and J. R. Gardinier, *Polyhedron*, 2004, **23**, 291.
8 D. L. Reger, K. J. Brown, J. R. Gardinier and M. D. Smith, *Organometallics*, 2003, **22**, 4973.
9 A. Lorenzotti, F. Bonati, A. Cingolani, G. G. Lobbia, D. Leonesi and B. Bovio, *Inorg. Chim. Acta*, 1990, **170**, 199.
10 J. L. Shaw, T. B. Cardon, G. A. Lorigan and C. J. Ziegler, *Eur. J. Inorg. Chem.*, 2004, 1073.
11 C. C. Chou, C. C. Su, H. L. Tsai and K. H. Lii, *Inorg. Chem.*, 2005, **44**, 628.
12 L. Zhang, M. Du, L. F. Tang, X. B. Leng and Z. H. Wang, *Acta Crystallogr., Sect. C*, 2000, **56**, 1210.
13 R. T. Stibrany, S. Knapp, J. A. Potenza and H. J. Schugar, *Inorg. Chem.*, 1999, **38**, 132.
14 K. A. Van Langenberg, B. Moubaraki, K. S. Murray and E. R. T. Tiekink, *Z. Kristallogr.-New Cryst. Struct.*, 2003, **218**, 345.
15 B. Kozlevcar, P. Gamez, R. de Gelder, W. L. Driessen and J. Reedijk, *Eur. J. Inorg. Chem.*, 2003, 47.
16 T. C. Higgs, D. Ji, R. S. Czernuscewicz and C. J. Carrano, *Inorg. Chim. Acta*, 1988, **273**, 14.
17 T. Astley, A. J. Canty, M. A. Hitchman, G. L. Rowbottom, B. W. Skelton and A. H. White, *J. Chem. Soc., Dalton Trans.*, 1991, 1981.
18 J. L. Shaw, G. T. Yee, G. Wang, D. E. Benson, C. Gokdemir and C. J. Ziegler, *Inorg. Chem.*, 2005, **44**, 5060.
19 Y. Xu, H. X. Li, W. H. Zhang, Y. Zhang and J. P. Lang, *Acta Crystallogr., Sect. C*, 2005, **61**, m4.
20 L. Zhang, W. M. Bu, S. P. Yan, Z. H. Jiang, D. Z. Liao and G. L. Wang, *Polyhedron*, 2000, **19**, 1105.
21 C. C. Chou, C. C. Su and A. Yeh, *Inorg. Chem.*, 2005, **44**, 6122.
22 H. V. R. Dias and H. Lu, *Inorg. Chem.*, 2000, **39**, 2246.
23 J. L. Shaw, T. B. Cardon, G. A. Lorigan and C. J. Ziegler, *Eur. J. Inorg. Chem.*, 2004, 1073.
24 C. Chou, C. Su, H. Tsai and K. Lii, *Inorg. Chem.*, 2005, **44**, 628.
25 C. M. Hartshorn and P. J. Steel, *Inorg. Chem.*, 1996, **35**, 6902.
26 C. M. Hartshorn and P. J. Steel, *J. Chem. Soc., Dalton Trans.*, 1998, 3927.
27 A. Omary, M. A. Rawashdeh-Omary, H. V. K. Diyabalanage and R. Dias, *Inorg. Chem.*, 2003, **42**, 8612.
28 D. L. Reger, R. P. Watson, J. R. Gardinier and M. D. Smith, *Inorg. Chem.*, 2004, **43**, 6609.
29 E. R. Humphrey, Z. Reeves, J. C. Jeffery, J. A. McCleverty and M. D. Ward, *Polyhedron*, 1999, **18**, 1335.
30 R. P. Feazell, C. E. Carson and K. K. Klausmeyer, *Eur. J. Inorg. Chem.*, 2005, 3287.
31 O. Crespo, E. J. Fernández, M. Gil, M. C. Gimeno, P. G. Jones, A. Laguna, J. M. López-de-Luzuriaga and M. E. Olmos, *J. Chem. Soc., Dalton Trans.*, 2002, 1319.
32 P. Ovejero, M. Cano, J. A. Campo, L. V. Heras, A. Laguna, O. Crespo, E. Pinilla and M. R. Torres, *Helv. Chim. Acta*, 2004, **85**, 2065.
33 R. G. Parr and W. Yang, *Density Functional Theory of Atoms and Molecules*, Oxford University Press, New York, 1989.
34 (*a*) G. te Velde, F. M. Bickelhaupt, S. J. A. van Gisbergen, C. Fonseca Guerra, E. J. Baerends, J. G. Snijders and T. Ziegler, Chemistry with ADF, *J. Comput. Chem.*, 2001, **22**, 931; (*b*) C. Fonseca Guerra, J. G. Snijders, G te Velde and E. J. Baerends, *Theor. Chem. Acc.*, 1998, **99**, 391; (*c*) ADF2005.01, SCM, Theoretical Chemistry, Vrije Universiteit, Amsterdam, The Netherlands, http://www.scm.com.
35 S. Abuskhuna, J. Briody, M. McCann, M. Devereaux, K. Kavanagh, J. B. Fontecha and V. McKee, *Polyhedron*, 2004, **23**, 1249.
36 (*a*) I. Mayer, *Chem. Phys. Lett.*, 1983, **97**, 270; (*b*) I. Mayer, *Int. J. Quantum Chem.*, 1984, **26**, 151.
37 C. M. Hartshorn and P. J. Stell, *J. Chem. Soc., Dalton Trans.*, 1998, 3935.
38 G. J. Kubas, *Inorg. Synth.*, 1979, **19**, 90.

39 R. Usón, A. Laguna, M. U. de la Orden and M. L. Arrese, *Synth. React. Inorg. Met.-Org. Chem.*, 1984, **14**, 369.
40 M. Bardají, O. Crespo, A. Laguna and A. K. Fischer, *Inorg. Chim. Acta*, 2000, **304**, 7.
41 J. Elguero, C. Ochoa, S. Julia, J. del Mazo, M. Sancho, J. P. Fayet and M. C. Vertut, *J. Heterocycl. Chem.*, 1982, **19**, 1141.
42 G. M. Sheldrick, *SHELXL-97, a Program for Crystal Structure Refinement*, University of Göttingen, Germany, 1997.
43 (*a*) L. Versluis and T. Ziegler, *J. Chem. Phys.*, 1988, **88**, 322; (*b*) L. Fan and T. J. Ziegler, *J. Chem. Phys.*, 1991, **95**, 7401.
44 S. H. Vosko, L. Wilk and M. Nusair, *Can. J. Phys.*, 1980, **58**, 1200.
45 J. P. Perdew, J. A. Chevary, S. H. Vosko, K. A. Jackson, M. R. Pederson, D. J. Singh and C. Fiolhais, *Phys. Rev. B*, 1992, **46**, 6671.
46 E. van Lenthe, A. Ehlers and E. J. Baerends, *J. Chem. Phys.*, 1999, **110**, 8943.
47 S. Portmann and H. P. Lüthi, *Chimia*, 2000, **54**, 766.